(see, for example, the very high temperature and high SiO_2 content of immiscible liquids in the system forsterite-silica in fig. 12.8). An experimentally known example of silicate liquid immiscibility that may have a natural analog is in the system fayalite (Fe_2SiO_4)-leucite ($KAlSi_2O_6$)-silica. This two-liquid field is a reasonable compositional analog for immiscibility observed in some uncommon dike rocks (lamprophyres) and some residual liquids formed during the last stages of basalt crystallization (*mesostasis*). It is unlikely, however, that silicate liquid immiscibility produces large volumes of differentiated magmas, because these compositions are only produced near the end of fractional crystallization sequences, when little liquid is left.

Liquid immiscibility seems to be most effective when the structures of the two melts are radically different. This can be achieved most readily if melt components with nonsilicate compositions are considered. One important example involves the separation of carbonate and silicate melts in CO_2-bearing systems. A photomicrograph of carbonatite globules suspended in alkali basalt is illustrated in figure 12.19. Immiscibility in such systems has been documented experimentally and almost certainly accounts for the production of the carbonatite magmas that are sometimes associated with alkalic silicate magmas. Another example is the separation of immiscible sulfide melts from basaltic magmas on cooling. The sulfide melts are more dense than silicate magma and readily sink. This may be an important mechanism for producing some sulfide ore deposits.

FIG. 12.19. Photomicrograph of immiscible carbonatite globu in alkali basalt. Two globules are coalescing. This sample is fr the Kaiserstuhl volcanic complex, Germany. Width of the photo graph is ~4 mm.

THE BEHAVIOR OF TRACE ELEMENTS

Much of the gemstone industry depends on the chance incorporation of minute quantities of certain elements into otherwise "ho-hum" minerals. Small proportions of foreign impurities can turn ordinary corundum into valuable rubies or sapphires. For the geochemist, elements present in trace concentrations can serve another purpose—to test and quantify geochemical models.

Trace elements are commonly defined as those occurring in rocks in concentrations of a few tenths of a percent or less by weight. The mixing behavior of trace components in crystals or melts is often highly nonideal; consequently, different minerals may concentrate or exclude trace elements much more selectively than they do major elements. Trace element distributions can therefore provide quantitative constraints on the proce of partial melting and differentiation that cannot deduced from consideration of major elements.

Trace Element Fractionation during Melting and Crystallization

In melt-crystal systems under equilibrium conditic elements are partitioned among phases according to tl activities in those phases. For trace elements, we n mally assume Henry's Law behavior, $a_i = h_i X_i$. The *tribution coefficient*, K_D, derived in chapter 9, is given K_D = concentration in mineral/concentration in liqu Trace element distribution coefficients are based on assumption that the trace component obeys Henr Law in the phase of interest. Experimental studies su gest that the linear Henry's Law region for many tra elements extends at least to several wt %, so it is app

cable for the concentration ranges measured in natural rocks. In principle, K_D can be measured from partially crystalline experimental charges or from natural lavas containing phenocrysts and glass. Many of the available distribution coefficients were determined from natural rocks, but there is unfortunately no assurance that these rocks reached equilibrium. There are also analytical problems in obtaining concentrates of pure phases (that is, crystals with no adhering or included glass, and vice versa), because trace elements are sometimes below the detection limits for in situ measurements. Another problem with K_D values is that they are dependent on the compositions of the phases. In other words, their distributions are nonideal, and enough information to determine the appropriate activity coefficients is usually not in hand. Despite these potential pitfalls, distribution coefficients are widely used to solve geochemical problems, and their compositional dependence can be minimized by selecting K_D values for phases similar in composition to those in the problem of interest.

The *bulk distribution coefficient* D is the K_D value adjusted for systems containing more than one solid phase. It is calculated from the weight proportions ω of each mineral ϕ by:

$$D = \sum \omega_\phi K_{D\phi}. \tag{12.3}$$

D must be calculated if we intend to handle models for partial melting of mantle peridotite or for fractionation of several minerals. Using the bulk distribution coefficient, we can predict trace element distributions during various magmatic processes.

We now derive expressions that describe changes in the concentrations of trace elements during solidification of a magma. We consider two ideal cases: equilibrium crystallization and perfect fractional crystallization (the latter is sometimes called *Rayleigh fractionation*). We assume that more than one phase is crystallizing.

In the case in which equilibrium between crystals and liquid is maintained,

$$X_{i\,\text{solid}}/X_{i\,\text{melt}} = D. \tag{12.4}$$

If a fraction of magma crystallizes, the fraction of melt remaining F is given by:

$$F = n_{\text{melt}}/n^0_{\text{melt}}, \tag{12.5}$$

where n^0_{melt} is the number of moles of all components in the original magma and n_{melt} is the total number of moles remaining after crystallization commences. The ratio of solid to melt remaining is therefore:

$$(n^0_{\text{melt}} - n_{\text{melt}})/n_{\text{melt}} = 1/F - 1. \tag{12.6}$$

If we define y_i as the number of moles of trace component i in the system, equations 12.4 and 12.6 can be combined to give:

$$\begin{aligned} X_{i\,\text{solid}}/X_{i\,\text{melt}} &= [y_{i\,\text{solid}}/(n^0_{\text{melt}} - n_{\text{melt}})]/(y_{i\,\text{melt}}/n_{\text{melt}}) \\ &= D. \end{aligned}$$

Because $y_{i\,\text{solid}} = y^0_{i\,\text{melt}} - y_{i\,\text{melt}}$,

$$D = [(y^0_{i\,\text{melt}}/y_{i\,\text{melt}}) - 1][(n_{\text{melt}}/(n^0_{\text{melt}} - n_{\text{melt}})].$$

Rearranging and dividing by $n^0_{\text{melt}}/n_{\text{melt}}$ gives:

$$\begin{aligned} (y^0_{i\,\text{melt}}/n^0_{\text{melt}})/(y_{i\,\text{melt}}/n_{\text{melt}}) = \\ \{D[(n^0_{\text{melt}} - n_{\text{melt}})/n_{\text{melt}}] + 1\}n/n^0. \end{aligned}$$

Substituting equation 12.5 into the expression above yields:

$$X_{i\,\text{melt}}/X^0_{i\,\text{melt}} = 1/(D - FD + F). \tag{12.7}$$

Expression 12.7 gives the concentration of trace element i in the liquid as a function of the original concentration, the bulk distribution coefficient, and the fraction of liquid remaining for a system undergoing equilibrium crystallization. The same expression also holds for equilibrium melting.

Now let's see how this differs from fractional crystallization. Using the same symbols as above, the mole fraction of trace component i in the system is $X_i = y_i/n$. If fractionation of a mineral containing i occurs, then n becomes $n - dn$, and y becomes $y - dy$. The compositions of solid and melt are therefore:

$$X_{i\,\text{solid}} = dy/dn \tag{12.8a}$$

and

$$X_{i\,\text{melt}} = (y - dy)/(n - dn). \tag{12.8b}$$

If trace component i obeys Henry's Law, then:

$$X_{i\,\text{solid}} = dy/dn = D\,X_{i\,\text{melt}}. \tag{12.9}$$

However, dy/dn can also be expressed in terms of $X_{i\,\text{melt}}$. If we neglect dy in comparison with much larger y and dn in comparison with n in equation 12.8b, we see that $X_{i\,\text{melt}}$ can be approximated as y/n and y as $n(X_{i\,\text{melt}})$.

Differentiating the latter expression with respect to n gives:

$$dy/dn = n(dX_{i\,\text{melt}}/dn) + X_{i\,\text{melt}}.$$

Substitution of this expression for dy/dn into equation 12.9 gives:

$$DX_{i\,\text{melt}} = n(dX_{i\,\text{melt}}/dn) + X_{i\,\text{melt}},$$

which can be recast into the form:

$$(1/X_{i\,\text{melt}}[D - 1])\, dX_{i\,\text{melt}} = (1/n)\, dn. \qquad (12.10)$$

Because X_i changes during crystallization, but not necessarily linearly, the way we obtain the total change in concentration is to sum all the individual steps. In other words, we integrate equation 12.10 between X_i^0 and X_i and between the initial and final moles of melt n^0 and n:

$$\ln(n/n^0) = [1/(D - 1)]\, \ln(X_{i\,\text{melt}}/X^0_{i\,\text{melt}}),$$

or

$$X_{i\,\text{melt}}/X^0_{i\,\text{melt}} = (n/n^0)^{D-1}.$$

Because (n/n^0) equals F, the fraction of liquid remaining:

$$X_{i\,\text{melt}}/X^0_{i\,\text{melt}} = F^{D-1}. \qquad (12.11)$$

Thus equations 12.7 and 12.11 describe the behavior of trace elements under the extreme conditions of equilibrium and fractional crystallization, respectively.

Using the same principles, analogous expres can be derived for partial melting models. These are here without derivation. For equilibrium melting:

$$X_{i\,\text{melt}}/X^0_{i\,\text{solid}} = 1/(D - FD + F), \qquad (12.1$$

and for fractional melting:

$$X_{i\,\text{melt}}/X^0_{i\,\text{solid}} = 1/D(1 - F)^{(1/D)-1}. \qquad (12.1$$

Because fractional melting involves continuous rem of melt as it is generated, this process probably not occur in nature, but it can be considered as an member for intermediate melting processes. Geocher models for magma generation have become very c plex and are beyond the scope of this book; Shaw (1 gives an excellent account of this topic.

The equations we have just derived can be expre equally well in units of concentration other than r fractions, as long as the distribution coefficients are fined in the same terms. In fact, most trace element ar ses are expressed in units of weight, for example, p per million (ppm), and we can substitute these con tration units for mole fractions in equations 12.7 12.11 if D is expressed as a weight ratio.

The changes in trace element concentration residual liquids under equilibrium and fractional cry lization are illustrated graphically in figure 12.20. Cu

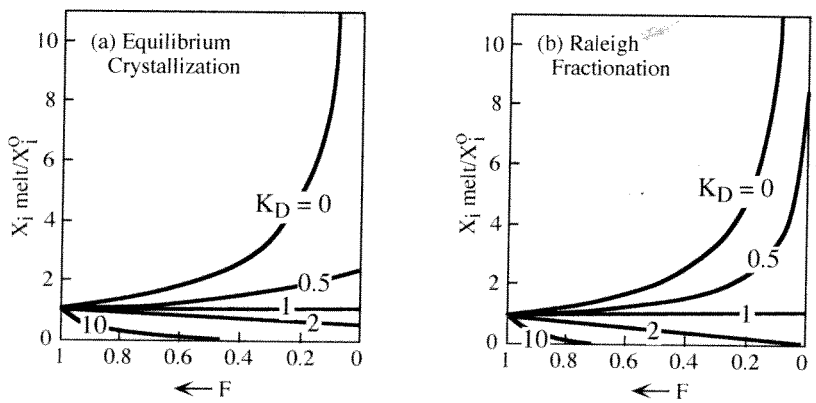

FIG. 12.20. Changes in trace element concentrations in residual liquids for different values of K_D during (a) equilibrium crystallization and (b) Rayleigh fractionation. Element concentrations are given in terms of mole fractions of each element i relative to its concentration in the parent magma. F is the fraction of liquid remaining. (After Wood and Fraser 1977.)

labeled $K_D = 0$ are limiting cases, and trace element enrichments greater than these cannot be produced by crystallization processes alone.

Compatible and Incompatible Elements

Earlier, we noted that it is useful to distinguish between trace elements that are compatible in the crystallographic sites of minerals and those that are incompatible with such minerals. Compatible elements have $K_D \gg 1$, whereas incompatible elements have $K_D \ll 1$. Consequently, compatible elements are preferentially retained in the solid residue on partial melting or extracted from the liquid during fractional crystallization; incompatible elements exhibit the opposite behavior. This can readily be seen in figure 12.20. Of course, as new minerals begin to melt or crystallize during the evolution of a magma, a particular trace element may alter its behavior. For example, phosphorus may act as an incompatible element during magmatic crystallization until the point at which the phosphate mineral apatite starts to form, after which it behaves compatibly. For applications involving mantle-derived magmas, it is often convenient to define compatible and incompatible behavior in terms of the minerals that make up mantle rocks—olivine, pyroxenes, garnet, and spinel. Incompatible elements are generally those with ionic radii too large to substitute for the more abundant elements, or those with charges of +3 or higher.

PREDICTING TRACE ELEMENT BEHAVIOR: TRANSITION METALS AND RARE EARTH ELEMENTS

Chemical physics provides powerful ways to predict trace element behavior. We illustrate this approach by considering several types of *transition elements,* which are characterized by inner d or f atomic orbitals that are incompletely filled by electrons. Unpaired electrons in transition elements are responsible for the distinctive colors of the minerals that contain them, as well as the magnetism of minerals. First we see how chemical bonding models can predict relative distribution coefficients.

Elements of the first transition series (Sc, Ti, V, Cr, Mn, Fe, Co, Ni, and Cu) have incompletely filled 3d orbitals, and cations are formed when the 4s and some 3d electrons are removed. Divalent ions in this series are compatible in common ferromagnesian minerals because of similarities to Mg^{2+} in ionic size and charge. However, the degree of compatibility differs markedly and can be explained by the effect of crystal structure on d orbitals. Crystal-field theory assumes that electrostatic forces originate from the anions surrounding the crystallographic site in which a transition metal ion may be located, and that these control its substitution in the structure.

A transition metal ion has five 3d orbitals, which have different spatial geometries (illustrated in fig. 2.7). In an isolated ion, the d electrons have equal probability of being located in any of these orbitals, but they attempt to minimize electron repulsion by occupying orbitals one electron at a time. For ions with more than five d electrons, this is obviously not possible, so a second electron can be added to each orbital by reversing its spin.

When a transition metal ion is placed in a crystal (for example, in octahedral coordination with surrounding anions), the five 3d orbitals are no longer degenerate; that is, they no longer have the same energy. Electrons in all five orbitals are repelled by the negatively charged anions, but electrons in the d_{z^2} and $d_{x^2-y^2}$ orbitals, which are oriented parallel to bonds between the cation and the anions around it, are affected to greater extent than those in the other three. In octahedral coordination, therefore, these two orbitals will have a higher energy level. The reverse is true for ions in tetrahedral coordination.

The energy separation between the two groups of orbitals is called *crystal-field splitting.* This is illustrated in figure 12.21. Ions with electrons in only the lower-energy orbitals for a particular site geometry are stable in that site, whereas electrons in the higher-energy orbitals destabilize the ion. Of course, the number of electrons depends on which transition metal the cation is made from and on its oxidation state, so some transition elements prefer octahedral sites more than others do. For example, the predicted octahedral site preference energies for divalent cations decrease in the order Ni > Cu > Co > Fe > Mn, and for

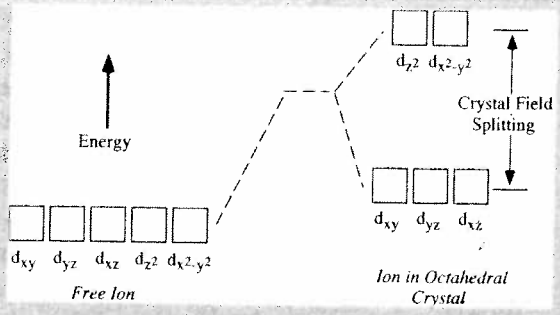

FIG. 12.21. Sketch of the energies of the five d orbitals in transition metal ions (refer to fig. 2.7 for geometric representations of these orbitals). When the free ion is placed in an octahedral mineral site, its total energy increases. Some orbitals have higher energy because they experience greater electron repulsion; the magnitude of the energy difference between the two groups of orbitals is the crystal-field splitting.

trivalent cations, Cr > V > Fe. As olivine or spinel (which offer octahedral sites) crystallizes from a magma, we expect to see rapid uptake of Ni and Cr in these minerals relative to other compatible transition metals. Tetrahedral sites in minerals produce a different but predictable order of cation site preferences. Thus, crystal-field effects provide an explanation for the differing K_D values for transition metals. The geochemical and mineralogical applications of crystal-field theory were treated comprehensively by Roger Burns (1970).

The lanthanide or *rare earth elements*, commonly abbreviated as REE, include La, Ce, Pr, Nd, Pm, Sm, Eu, Gd, Tb, Dy, Ho, Er, Tm, Yb, and Lu. The REEs find wide application in metallurgy, the coloring of glass and ceramics, and the production of magnets. In this part of the periodic table, increasing atomic number adds electrons to the inner 4f orbitals, so this is a somewhat similar case to the transition metals just discussed. The f electrons in REE, however, do not participate in bonding. The valence electrons occur in higher-level orbitals, and loss of three of these results in a +3 charge for most REE cations. These are large ions; their size, coupled with their high charges, makes them incompatible.

Europium (Eu) is unique in that its third valence electron does not enter the 5d orbital as in other REEs, but a 4f orbital, which then becomes exactly half full. This is a particularly stable configuration, and m energy is required to remove the third electron consequence of this is that under reducing conditic such as on the Moon or within the Earth's man Eu may exist in both the divalent and trivalent st (the ratio of Eu^{2+} and Eu^{3+} depends on the oxidat state of the system). Eu^{2+} has about the same size a charge as Ca^{2+}, for which it readily substitutes, europium, at least in part, may behave as a comp ible element.

Under oxidizing conditions, such as in the mar environment, cerium (Ce) is oxidized to Ce^{4+}. T results in a significant contraction in its ionic radi thus, Ce^{4+} has a very different behavior from trivale ions of the other REEs. Cerium in the oceans preci tates in manganese nodules, consequently leading t dramatic Ce depletion in seawater. Marine carbona formed in this enviroment mimic this geochemic characteristic. Metalliferous sediments deposited midocean ridges also exhibit Ce depletions, pointi to a seawater source for the hydrothermal solutio that produced them.

The natural abundances of REEs vary by a fact of thirty. To simplify comparisons, REE concentratio in rocks are normalized by dividing them by the concentrations in another rock sample. Chondrit meteorites, which are thought to contain unfractio ated element abundances, are the most commonly use standard for REE normalization. The geochemic significance of these meteorites is considered in cha ter 15. Shales also generally have uniform lanthanic patterns, and several sets of shale REE abundances a used for normalization in some applications. As w have already discussed earlier in this chapter, shale have geochemical significance because their composi tions may represent that of the average crust. Nor malization of REE data using chondritic meteorites o shales produces relatively smooth patterns that enabl comparisons between samples, accentuating relativ degrees of enrichment or depletion and contrastin behavior between neighboring elements in the lan thanide series. Normalized REE concentrations ar conventionally shown in diagrams such as that showr in figure 12.22, plotted by increasing atomic number The elements on the left side of the diagram thus have lower atomic weights and are called the light rare

earth elements (LREE) to distinguish them from their heavier counterparts (HREE) on the right. What is important from the standpoint of geochemical behavior, however, is that the lanthanides show a regular contraction in ionic radius from La^{3+} to Lu^{3+}.

Except for Eu^{2+} in reduced systems and Ce^{4+} in oxidized systems, the REEs are all incompatible but, like the first series transition metals, their behavior varies in degree. Some minerals can tolerate certain REEs more easily than others, as shown in figure 12.22. For example, apatite can readily accommodate all rare earth elements. Some minerals discriminate between different rare earth elements, resulting in their fractionation. Garnet has a phenomenal preference for HREEs because of their smaller ionic radii, and pyroxenes show a similar but less pronounced affinity. The extra Eu in plagioclase, accounting for the spike or *positive europium anomaly,* is Eu^{2+} substituting for calcium. Thus K_D values for the REEs in various phases are controlled by size rather than by bonding characteristics.

Studies of REEs have found many uses in geochemistry. They constitute important constraints on models for partial melting in the mantle and magmatic fractionation. The lanthanides are insoluble under conditions at the Earth's surface, so their abundances in sediments reflect those of the average crust. The short residence times for REEs in seawater also allow them to be used to track oceanic mixing processes. More exhaustive treatments of REE geochemistry can be found in Henderson (1983) and Taylor and McLennan (1987).

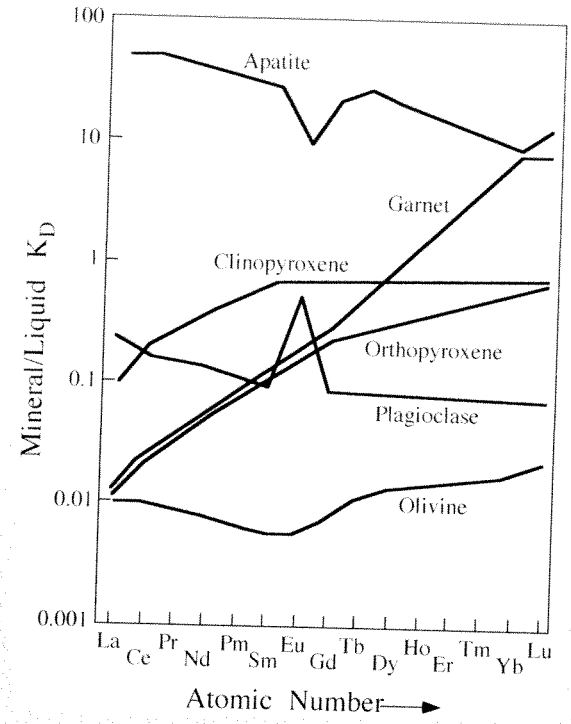

FIG. 12.22. Typical distribution coefficients for REEs between various minerals and basaltic melt. REE concentrations are normalized to values in chondritic meteorites. All of these phases are intolerant of REE (that is, $K_D < 1$) except apatite (and garnet for the HREEs). The positive Eu anomaly in plagioclase occurs because some of this element is in the divalent state and can substitute for Ca^{2+} ions. (After Zielinski 1975.)

A knowledge of compatible and incompatible trace element distribution coefficients can provide a powerful test for geochemical models involving partial melting or crystallization. Some representative K_D values for trace elements in minerals in equilibrium with basaltic magma are presented in table 12.4. An example of such a test is given in worked problem 12.8.

We are now in a position to evaluate how the crust-mantle system has become stratified in terms of its heat-producing radioactive elements. Potassium, uranium, and thorium are all very large ions and behave as incompatible elements. Consequently, any partial melts produced in the mantle scavenges these elements, and over time, they become depleted from mantle residues and concentrated in the crust by ascending magmas. This differentiation of heat-producing elements has had a profound effect on the Earth's thermal history.

Worked Problem 12.8

How can trace element abundances in basalts be used to constrain models for their origin? A geochemical study of volcanic

TABLE 12.4. Representative Trace Element K_D Values for Minerals in Equilibrium with Basaltic Magma

Mineral	Ni	Rb	Sr	Ba	Ce	Sm	Eu	Y
Olivine	10	0.001	0.001	0.001	0.001	0.002	0.002	0.002
Clinopyroxene	2	0.001	0.07	0.001	0.1	0.3	0.2	0.3
Orthopyroxene	4	0.001	0.01	0.001	0.003	0.01	0.01	0.05
Garnet	0.04	0.001	0.001	0.002	0.02	0.2	0.3	4.0
Amphibole	3	0.3	0.5	0.4	0.2	0.5	0.6	0.5
Plagioclase	0.01	0.07	2.2	0.2	0.1	0.07	0.3	0.03

From Cox et al. (1979).

rocks from Reunion Island in the Indian Ocean by Robert Zielinski (1975) provides an excellent example. Measured trace element abundances in eight samples are shown in figure 12.23. All of these samples contain phenocrysts of olivine, clinopyroxene, plagioclase, and magnetite in a groundmass of the same minerals plus apatite. Zielinski used the major element compositions of whole rocks and phenocrysts to construct a fractionation model. Using a petrologic mixing program, he found that lava samples 3–8 could be formed by fractionation of these phenocrysts from assumed parental magma 2. Basalt 1 was not a suitable parental magma for this suite, even though it has the highest Mg/Fe ratio; this rock probably contains cumulus olivine and pyroxene. Zielinski then tested this model using trace elements.

The chondrite-normalized rare earth element patterns (fig. 12.23a) are parallel and increase in the order sample 1 to 8. This is just as expected; incompatible REEs should have higher concentrations in residual liquids, and none of the solid phases fractionates LREEs from HREEs appreciably. Using the K_D values shown in figure 12.22 and the proportions of fractionating phases from the mixing program, it is possible to calculate the bulk distribution coefficient (equation 12.3) for each sample. The mixing program also gives the fraction of liquid F. Assuming equilibrium between the entire separated solid and melt, substitution of these values into equation 12.7 gives the ratio $C_{i\ \text{melt}}/C^0_{i\ \text{melt}}$. Assume, as Zielinski did, that rock 2 is the parental magma; its trace element concentrations are then $C^0_{i\ \text{melt}}$. Thus, we can calculate the expected REE pattern for liquids derived from sample 2. When Zielinski did this exercise, he was able to duplicate the measured REE patterns fairly accurately. The negative Eu anomaly in rock 8 is caused by the removal of large quantities of plagioclase at the end of the crystallization sequence.

The abundances of some other trace elements in these rocks are shown in figure 12.23b. Uranium and thorium are even more incompatible than REEs and increase progressively in the sequence. Barium is also incompatible, but it and strontium can substitute in sodic plagioclase, so both drop towards the end of the sequence as feldspar fractionation becomes dominant. In

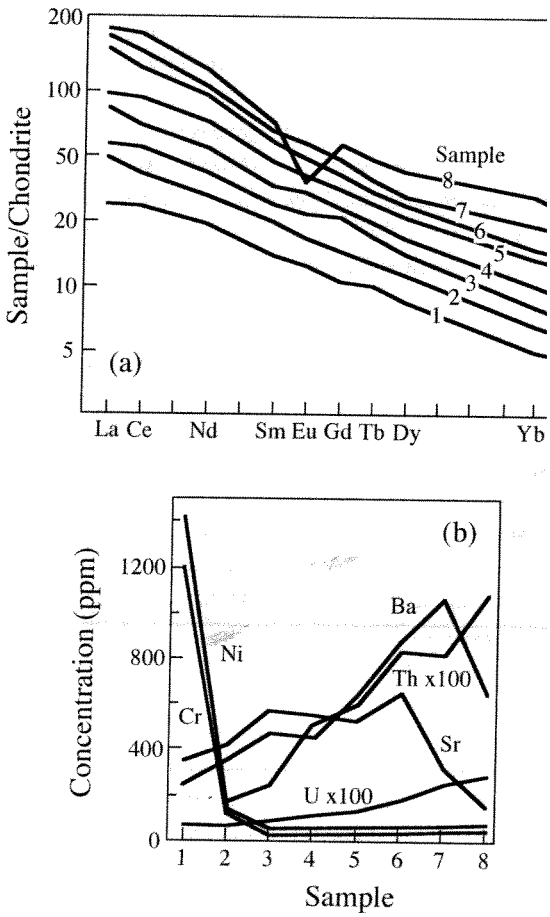

FIG. 12.23. Chondrite-normalized REE patterns (a) and other trace element variations (b) for a suite of volcanic rocks analyze by Zielinski (1975). The patterns are consistent with a model whereby samples 3–8 were formed by progressive fractional crystallization of a liquid having the composition of sample 2. Sample 1 appears to be a cumulate rock.

contrast, nickel and chromium are compatible and show marked depletions in fractionated rocks. Their contents in rock 1 are much higher than expected for a primary magma, and this observation lends support to the idea that this rock contains cumulus phases. Using appropriate D and F values, we could also predict the abundances of these elements in the hypothetical fractionation sequence. Zielinski was also able to model these fairly well.

Even though Zielinski's modeling may appear convincing, we should note that this is not a unique solution to this problem. The same geochemical patterns might also be produced by various degrees of partial melting of mantle peridotite. Rock 8 would represent a magma formed during a small amount of melting. As melting advanced, the incompatible elements in the melt phase would be progressively diluted, ultimately to produce magma 2. Actually, Zielinski recognized this possibility, but argued against it on the basis of field evidence for shallow differentiation. Like many other tools of geochemistry, trace element modeling may give ambiguous answers, and is at its best when used in combination with other investigative methods.

VOLATILE ELEMENTS

The crust and mantle also interact geochemically by the exchange of volatile elements. Hydrogen, oxygen, carbon, sulfur, and other volatiles in the Earth's interior may be bound into crystal structures, dissolved in magmas, or exist as a discrete fluid phase. We use the term *fluid* because P-T conditions in the mantle and crust are such that this phase is generally above its critical point, where the distinction between liquid and gas is meaningless. Before we can investigate how fluids are cycled within the planet's interior, we should examine their compositions.

Crust and Mantle Fluid Compositions

The compositions of fluids in the crust and mantle can be ascertained from several different lines of evidence. The first is direct chemical analysis of waters from deep wells in geothermal fields such as the Salton Sea, California. In chapter 7, we showed how computer programs such as EQ6 can be used to model the chemical evolution of natural waters. Such sophisticated methods have been used to verify that the measured compositions of these fluids are in equilibrium with the metamorphic minerals in core samples, supporting the idea that these are contemporary metamorphic fluids. It is often difficult, however, to assess the extent to which such fluids may have been contaminated by meteoric water or drilling muds, and sampling of fluids from depths of more than a few kilometers is out of the question.

Fluid inclusions trapped in the minerals of crustal and mantle rocks (both igneous and metamorphic) provide another method of direct observation. Although these inclusions contain only minute quantities of fluids, they can sometimes be extracted for chemical analysis. More commonly, their compositions are inferred from heating and freezing experiments in situ. The experimental manipulation of fluid inclusions in considered further in an accompanying box.

EXTRACTING INFORMATION FROM FLUID INCLUSIONS

Fluids are commonly stranded in interstitial spaces as minerals crystallize. They may be trapped along old crystal boundaries, in fractures, or within pore spaces. With time, these interstitial spaces gradually change shape to minimize their surface energies. The result is a population of more or less equally dimensioned spherical fluid inclusions. Because the minimal surface energy may be best attained by adapting inclusion shape to the structure of the host mineral, some inclusions have *negative crystal* shapes. At the time of trapping, the fluid is usually a single phase liquid or supercritical fluid. The fluid shrinks on cooling, because the coefficient of thermal expansion for the host mineral is much less than for the fluid. As the pressure in inclusions drops below the vapor pressure of the fluid components, vapor bubbles nucleate and grow. Most fluid inclusions, therefore, contain both a liquid and a vapor phase. Solid phases are also commonly encountered in inclusions that have become saturated with respect to one or more salts on cooling. These *daughter crystals* may be valuable clues to the compositions of the parent fluid. It is also common, particularly in sedimentary environments, to find inclusions containing a second, immiscible fluid (usually composed mostly of organic matter). Many of these features are illustrated in the inclusion